Journal of The Physical Society of Japan
Vol. 60, No. 6, June, 1991, pp. 1885–1889

Neutron Diffraction Study of $CuFeO_2$

Setsuo MITSUDA,* Hideki YOSHIZAWA, Nariyasu YAGUCHI† and Mamoru MEKATA†

Institute for Solid State Physics, University of Tokyo, Roppongi, Tokyo 106
†Department of Applied Physics, Faculty of Engineering, Fukui University, Bunkyo, Fukui 910

(Received April 12, 1991)

Neutron diffraction study revealed that a powdered $CuFeO_2$, a quasi-two-dimensional antiferromagnet on a triangular lattice (AFT), has two successive magnetic phase transitions at low temperatures. In the high-temperature phase below $T_{N1}=16$ K, it has a monoclinic magnetic unit cell with five spins in a layer ($\sqrt{7}a\times\sqrt{7}a\times 2c$, $\gamma=141.78°$). At $T_{N2}=10$ K, it shows a discontinuous transition and enters the low-temperature phase with an orthorhombic magnetic unit cell with four spins in a layer ($\sqrt{3}a\times 2a\times 2c$). In both magnetic structures, spins are collinear and parallel to the c axis.

The compound $CuFeO_2$ (delafossite) is a layered triangular lattice antiferromagnet where the triangular lattices of the magnetic Fe^{3+}, which are separated by nonmagnetic ion layers of Cu^+ and O^{2-}, stack in a sequence of A-B-C along the c axis. Its chemical structure belongs to the space group $R\bar{3}m$ and has cell parameters $a=3.03$ Å and $c=17.09$ Å in the hexagonal description.[1] From magnetic susceptibility measurements,[2] the Weiss temperature has been determined to be ~ -100 K, indicating that the dominant magnetic interaction is antiferromagnetic and is of the order of 100 K. Nevertheless, a rather low antiferromagnetic transition temperature $T_N\sim 16$ K $\ll 100$ K might suggest that there are strong geometrical frustrations characteristic to the triangular lattice with antiferromagnetic interactions. For such a frustrated magnetic system, competing magnetic interactions lead to a variety of magnetic orders. For example, complicated higher-order commensurate magnetic structures are predicted for an Ising antiferromagnet on a triangular lattice (AFT) with nearest and next-nearest-neighbor interactions.[3] The isostructural compounds $ACrS_2$ (A=Cu, Na, Li)[4] or $LiCrO_2$,[5] are known to show relatively complex helimagnetic structures. In the present paper, we report the magnetic structure of $CuFeO_2$ determined by neutron diffraction. In contrast to the isostructural compounds mentioned above, it turned out that $CuFeO_2$ has two magnetically ordered phases with higher-order commensurate magnetic structures at low temperatures.

We have performed neutron scattering experiments on the triple-axis spectrometer at JRR-2 JAERI (Tokai) in a double-axis configuration. The sample was mounted in a standard helium flow-type cryostat. The powder sample of $CuFeO_2$ was prepared by solid-state reaction ($Cu_2O+Fe_2O_3\longrightarrow 2CuFeO_2$), as described in ref. 2. An incident neutron with a wave number of $k_i=2.57$ Å^{-1} was obtained by pyrolytic graphite (PG) double monochromators with their (002) reflection. To suppress higher-order contaminations, a PG filter was used. Collimation of 40′-80′-80′-40′-open was employed.

Powder scans in the range of $5°<2\theta<80°$ were carried out at 50 K, 13.5 K and 4.6 K, corresponding to the paramagnetic ($T>T_{N1}$), intermediate ($T_{N1}>T>T_{N2}$), and low-temperature ($T_{N2}>T$) phases, respectively. The results in the interval of $10°<2\theta<50°$ are shown in Fig. 1. Asymmetric strong diffuse scattering was observed in the paramagnetic phase, as shown in Fig. 1(a), which indicates the two-dimensional character of this system. In the intermediate phase, the scattering intensity con-

* Present address: Department of Physics, Faculty of Science, Science University of Tokyo, Kagurazaka, Shinjuku-ku, Tokyo.

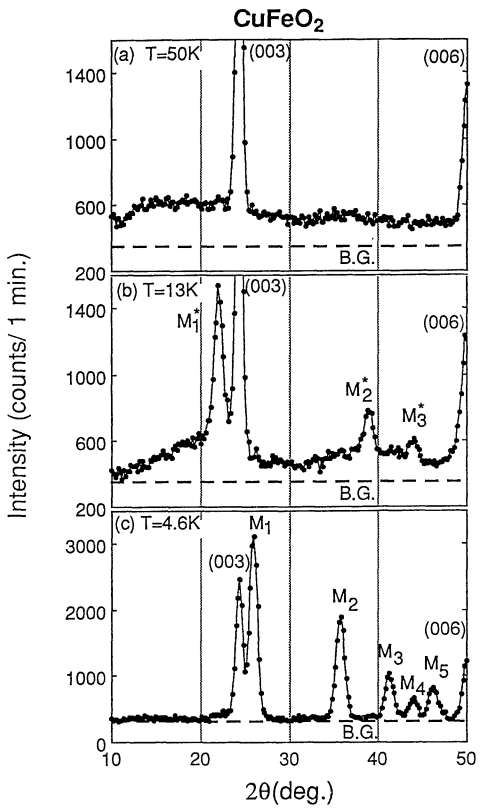

Fig. 1. Neutron diffraction pattern for powdered $CuFeO_2$ at T=(a) 50 K, (b) 13 K and (c) 4.6 K. Observed magnetic peaks labeled (M_1-M_5, M_1^*-M_3^*) are listed in Tables I and II.

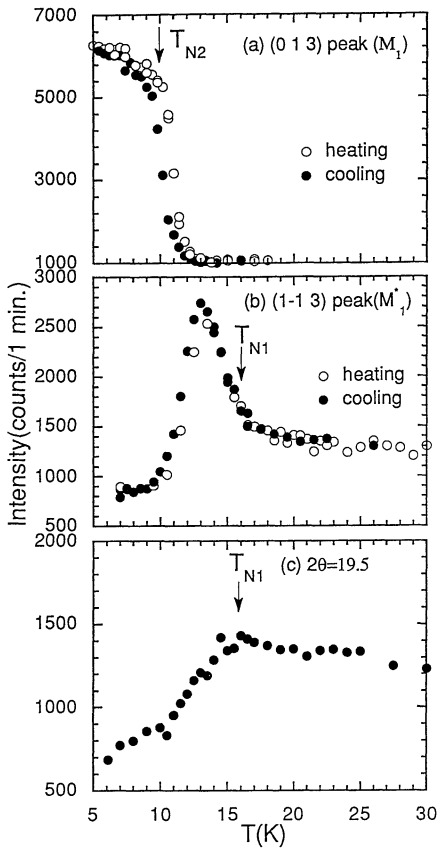

Fig. 2. Temperature dependence of intensity of (a) magnetic peak M_1, (b) magnetic peak M_1^* and (c) diffuse scattering at 2θ=19.5°.

sists of both diffuse scattering and a few weak magnetic Bragg peaks (labeled M_1^* to M_3^*), as seen in Fig. 1(b). In the low-temperature phase, several magnetic Bragg peaks (labeled M_1 to M_5) were observed, as shown in Fig. 1(c). To show the thermal evolution of the intermediate- and the low-temperature magnetic phases, the temperature dependence of the peak intensity of the Bragg reflections M_1^* and M_1, as well as diffuse scattering observed at 2θ=19.5°, are shown in Fig. 2. With decreasing temperature, the intensity of the M_1^* peak begins to increase at T=16 K where the diffuse scattering intensity shows its maximum. However, around T=11 K, while the intensity of the M_1^* peak decreases rapidly, the intensity of the M_1 peak increases with hysteresis, which indicates that $CuFeO_2$ has two magnetic phase transition temperatures, at T_{N1}=16 K and T_{N2}=11 K, of the second and the first orders, respectively.

As for chemical structure, we reproduced the integrated intensity of the observed nuclear peaks at T=50 K, where the R factor, defined by $R=\Sigma|I_{obs}-I_{cal}|/\Sigma I_{obs}$, is about 1.6% with only one adjustable parameter z_0=0.1063, the atomic position of oxygen (0, 0, z_0). Above and below T_{N2}, no detectable

Table I. Magnetic peaks in the low temperature phase (T=4.6 K). The calculated intensities are normalized to the observed one at (0, 1, 3) peak. Indexing of peaks is based on the orthorhombic notation.

Label	Index	$2\theta_{obs}$	$2\theta_{cal}$	Integrated obs.	Intensity cal.
M_1	(0, 1, 3)	26.12	26.12	29.6	29.6
M_2	(1, 1, 1)	35.74	35.74	18.1	18.6
M_3	(1, 1, 5)	41.25	41.26	7.8	9.9
M_4	(0, 1, 9)	43.94	44.10	3.2	3.2
M_5	(1, 1, 7)	46.23	46.23	5.8	6.1

Table II. Magnetic peaks in the intermediate temperature phase ($T=13$ K). The calculated intensities are normalized to the observed one at (1, −1, 3) peak. Indexing of peaks is based on the monoclinic notation. †Small humps can be seen but integrated intensity is hardly measured due to coexistence of strong diffuse scattering. ††Magnetic peak as strong as M_3^* peak is found by comparison between the profiles at $T=50$ K and 13 K.

Label	Index	$2\theta_{obs}$	$2\theta_{cal}$	Integrated Intensity$_{obs}$	Intensity$_{cal}$ model (a)	Intensity$_{cal}$ model (b)	Intensity$_{cal}$ model (c)	Intensity$_{cal}$ model (d)
M_1^*	(1, −1, 3)	22.09	22.10	11.1	11.1	11.1	11.1	11.1
†	(1, 0, 1)	—	28.53	—	1.3	65.7	9.5	0.49
†	(1, 0, 5)	—	35.05	—	0.53	29.9	4.3	0.21
M_2	(2, −1, −1)	38.80	39.05	3.2	4.1	5.41	5.4	4.34
†	(2, −2, 3)	—	39.32	—	0.54	33.3	4.8	0.22
†	(1, 0, 7)	—	40.65	—	0.28	17.2	2.5	0.11
†	(1, −1, 9)	—	41.69	—	0.75	0.98	0.98	0.75
M_3^*	(2, −1, 5)	44.0	44.22	1.4	2.5	3.4	3.4	2.5
††	(2, −1, −7)	~49	48.95	—	1.5	2.3	2.3	1.6

change of cell parameters was found within experimental accuracy. In contrast to the 120° magnetic structure widely found in continuous spin antiferromagnets with nearest-neighbor antiferromagnetic interaction, the observed magnetic peaks could not be assigned to indexes such as $(1/3, 1/3, l)$. Both integrated intensities I_{obs} and peak positions $2\theta_{obs}$ of these magnetic Bragg peaks in the low and intermediate phases are listed in Tables I and II, which are well explained in terms of magnetic structure models with an orthorhombic and a monoclinic unit cell, respectively, as will be discussed below.

In order to assign the observed magnetic peaks, we introduce the orthorhombic magnetic unit cell with lattice parameters ($a^o=\sqrt{3}a^h$, $b^o=2a^h$, $c^o=2c^h$) for the low-temperature phase and a monoclinic magnetic unit cell with lattice parameters ($a^m=\sqrt{7}a^h$, $b^m=\sqrt{7}a^h$, $c^m=2c^h$ and $\gamma=141.78°$) for the intermediate phase, as shown in Figs. 3(a) and 3(b), respectively. Note that the superscripts o, m and h refer to the orthorhombic, the monoclinic and the hexagonal notations, respectively. Both magnetic cells contain six magnetic triangular lattice layers (labelled by $j=1$ to 6) stacked along the c axis in a sequence of ABCABC. Each Fe^{3+} in the j-th layer which has normalized spin S_m^j, is labelled by $m=1$ to 4 or 5, and has the atomic position r_m^j which is listed in Table III. Since the Mössbauer study[6] on a single crystal of $CuFeO_2$ revealed that the spin direction is parallel to the c axis, we assume a simple collinear magnetic structure. Hence, the intensity of the magnetic Bragg reflection $I(hkl)$ is represented by eq. (1),

$$I(hkl) \propto q \sum_j \sum_m S_m^j \exp(i\boldsymbol{Q}\cdot\boldsymbol{r}_m^j), \qquad (1)$$

where q is the spin-orientation factor, and the normalized spin S_m^j takes +1 or −1 corresponding to the up or down spin direction with respect to the c axis.

First, let us consider the magnetic structure in the low-temperature phase. In Table I, we find the following three extinction rules:

(A) (h, k, l) reflections with l=even integer are not allowed;

Table III. Atomic positions of Fe in (a) orthorhombic and (b) monoclinic magnetic unit cells: Position vector r_m^j of j-th layer's m-th Fe atom in j-th layer is given by sum of the vectors r_m and δ^j which points to j-th layer. (i.e. $r_m^j=r_m+\delta^j$).

(a) Orthorhombic	(b) Monoclinic
r_1 (1, 0, 0)	r_1 (0, 0, 0)
r_2 (1/2, 1/4, 0)	r_2 (1/5, 4/5, 0)
r_3 (1, 1/2, 0)	r_3 (2/5, 3/5, 0)
r_4 (1/2, 3/4, 0)	r_4 (3/5, 2/5, 0)
	r_5 (4/5, 1/5, 0)
δ^1 (0, 0, 0)	δ^1 (0, 0, 0)
δ^2 (1/6, 1/4, 1/6)	δ^2 (1/15, 4/15, 1/6)
d^3 (−1/6, 1/4, 2/6)	δ^3 (1/3, 1/3, 2/6)
δ^4 (0, 0, 3/6)	δ^4 (0, 0, 3/6)
δ^5 (1/6, 1/4, 4/6)	δ^5, (1/15, 4/15, 4/6)
δ^6 (−1/6, 1/4, 5/6)	δ^6 (1/3, 1/3, 5/6)

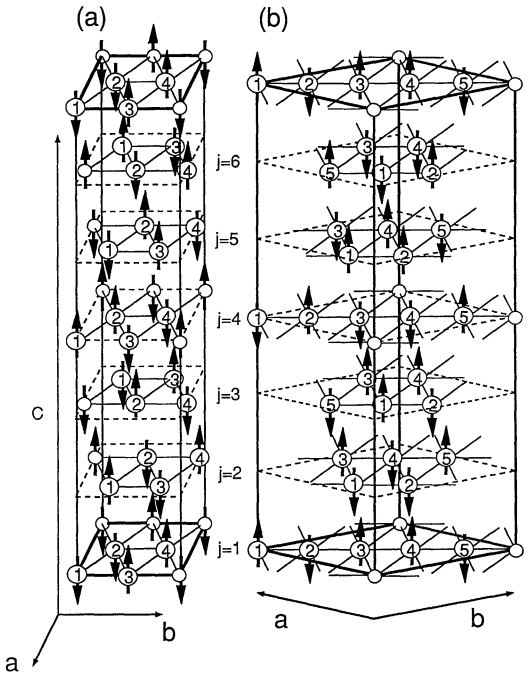

Fig. 3. Schematic drawing of magnetic structures determined for (a) low and (b) intermediate phases. The atomic position and the normalized spins are listed in Tables III, IV and V.

(B) $(1, 0, l)$ reflections are not allowed;

(C) $(0, 1, l)$ reflections with $L \neq 6n-3$ are not allowed (n is an integer).

To satisfy these extinction rules, we obtain the following conditions:

$$S_m^{j+3} = -S_m^j, \tag{2}$$

$$S_1^j - S_2^j + S_3^j - S_4^j = 0, \tag{3}$$

$$\arg(\Gamma^2 e^{2\pi i \frac{9}{12}}) = \arg(\Gamma^1) = \arg(\Gamma^3 e^{-2\pi i \frac{3}{12}}),$$

with

$$\Gamma^j \equiv S_1^j + iS_2^j - S_3^j - iS_4^j. \tag{4}$$

Using these conditions, it is shown that the only possible magnetic structure is the one whose S_m^j is listed in Table IV. The intensities of the magnetic reflections reproduced on the basis of this model are listed in Table I. A schematic drawing of the spin arrangement of the model is given in Fig. 3(a). The moment value extrapolated to 0 K is $4.0 \pm 0.2\,\mu_B$.

Next, let us consider the magnetic structure in the intermediate phase. In Table II, we find the following two extinction rules:

(A′) (h, k, l) reflections with l=even integer are not allowed;

(B′) $(2, -1, l)$ reflections with $l \neq 6n-1$ are not allowed.

These extinction rules lead to the following conditions:

$$S_m^{j+3} = -S_m^j, \tag{5}$$

$$\arg(\Phi^1) = \arg(\Phi^2 e^{2\pi i \frac{-9}{30}}) = \arg(\Phi^3),$$

with

$$\Phi^j \equiv S_1^j + e^{2\pi i \frac{3}{5}} S_2^j + e^{2\pi i \frac{1}{5}} S_3^j + e^{2\pi i \frac{4}{5}} S_4^j + e^{2\pi i \frac{2}{5}} S_5^j. \tag{6}$$

It is shown that there exist three possible magnetic structures which are consistent with the above conditions, as listed in Table V (a) through (c). By comparing the observed and the calculated intensities of the magnetic reflections for those models listed in Table II, we conclude that model (a) is the most probable magnetic structure for the intermediate phase, and its spin arrangement is shown schematically in Fig. 3(b). Here it should be noted that extinction rule B′ is not uniquely obtained from the diffraction pattern since two reflections (h, k, l) and $(h, k, -l)$ are not distinguishable due to powder averaging. However, there exists no solution in the case where one chooses the extinction rule counter to (B′), i.e., $(2, -1, l)$ reflections with $l \neq 6n+1$ are not allowed.

Recalling that one of this family of compounds, $CuCrO_2$, a Heisenberg spin AFT with $S=3/2$,[7] has 120° magnetic structure, it is surprising that the present sample $CuFeO_2$ shows the collinear magnetic structure. Since $CuFeO_2$ is also considered to be a Heisenberg spin AFT with $S=5/2$ of Fe^{3+} ions, as confirmed by the isomer shift in Mössbauer ex-

Table IV. Magnetic structure model for low-temperature phase where normalized spin S_m^j are shown as up (+) or down (−).

		j					
		1	2	3	4	5	6
m	1	−	+	−	+	−	+
	2	−	−	+	+	+	−
	3	+	−	+	−	+	−
	4	+	+	−	−	−	+

Table V. Magnetic structure models for intermediate-temperature phase where normalized spin S^j_m are shown as up (+) or down (−) or zero (0).

model (a)

m \ j	1	2	3	4	5	6
1	+	−	+	−	+	−
2	−	−	−	+	+	+
3	+	+	+	−	−	−
4	+	−	+	−	+	−
5	−	+	−	+	−	+

model (b)

m \ j	1	2	3	4	5	6
1	−	−	−	+	+	+
2	−	−	−	+	+	+
3	+	+	+	−	−	−
4	+	+	+	−	−	−
5	−	+	−	+	−	+

model (c)

m \ j	1	2	3	4	5	6
1	+	+	+	−	−	−
2	−	+	−	+	−	+
3	−	+	−	+	−	+
4	−	−	−	+	+	+
5	−	+	−	+	−	+

model (d)

m \ j	1	2	3	4	5	6
1	0	+	0	0	−	0
2	+	−	+	−	+	−
3	−	+	−	+	-	+
4	+	0	+	−	0	−
5	−	−	−	+	+	+

periments,[6] we have, at this moment, no straightforward explanation as to why the collinear structure is stabilized.

Finally, it should be noted that the strong diffuse scattering coexists with magnetic Bragg peaks in the intermediate-temperature phase. This may be explained by analogy with a partially disordered phase observed in the Ising spin AFT C_sCoCl_3[8] where diffuse scattering comes from a paramagnetic sublattice of the three sublattices in the partially disordered phase, and vanishes in the low-temperature ferrimagnetic phase. Owing to the frustration among the spins, partial disorder below T_{N1} is also expected in $CuFeO_2$. For instance, if we assume the partially disordered magnetic structure where one of five sublattices is paramagnetic, as in model (d) in Table V, the intensities of magnetic reflections are reproduced equally well, as in model (a). At the present stage, although both models are compatible with our data within experimental accuracy, it is likely that the partially disordered model is more suitable for the magnetic structure in the intermediate phase. Experiments using a single crystal are desired.

In conclusion, from neutron diffraction study on powdered $CuFeO_2$, it was revealed that $CuFeO_2$ has two collinear magnetic ordered phases with an orthorhombic and a monoclinic magnetic unit cell in contrast to the hexagonal 120° magnetic structure typical of Heisenberg spin AFT. More detailed discussion on the magnetic structure of $CuFeO_2$ will appear soon elsewhere.

We are grateful to Dr. H. Kadowaki for valuable discussions and to Mr. Y. Kawamura for his technical assistance.

Reference

1) A. Pabst: Am. Mineralogist **31** (1946) 539.
2) J. P. Doumerc, A. Wichainchai, A. Ammar, M. Pouchard and P. Hagenmuller: Mat. Res. Bull. **21** (1986) 745.
3) K. Nakanishi and H. Shiba: J. Phys. Soc. Jpn. **51** (1982) 2089.
4) F. M. R. Engelsman, G. A. Wiegers, F. Jellinck and B. van Laar: J. Solid State Chem. **6** (1973) 574.
5) J. L. Soubeyroux, D. Fruchart, J. C. Marmeggi, W. J. Fitzgerald, C. Delmas and G. Le Flem: Phys. Status Solidi **67** (1981) 663.
6) A. H. Muir, Jr. and H. Wiedersich: J. Phys. Chem. Solids **28** (1967) 65.
7) H. Kadowaki, H. Kikuchi and Y. Ajiro: J. Phys. Condens. Matter (1990).
8) M. Mekata and K. Adachi: J. Phys. Soc. Jpn. **44** (1978) 806.